Published online 28 February 2012 *Nucleic Acids Research, 2012, Vol. 40, No. 12* ***5577–5590***
doi:10.1093/nar/gks186

Microhomology-mediated DNA strand annealing and elongation by human DNA polymerases λ and β on normal and repetitive DNA sequences

Emmanuele Crespan[1], Tibor Czabany[2], Giovanni Maga[1,*] and Ulrich Hübscher[2]

[1]Institute of Molecular Genetics IGM-CNR, via Abbiategrasso 207, 27100 Pavia, Italy and [2]Institute of Veterinary Biochemistry and Molecular Biology, University of Zürich-Irchel, Winterthurerstrasse 190, 8057 Zürich, Switzerland

Received October 21, 2011; Revised February 2, 2012; Accepted February 6, 2012

ABSTRACT

'Classical' non-homologous end joining (NHEJ), dependent on the Ku70/80 and the DNA ligase IV/XRCC4 complexes, is essential for the repair of DNA double-strand breaks. Eukaryotic cells possess also an alternative microhomology-mediated end-joining (MMEJ) mechanism, which is independent from Ku and DNA ligase 4/XRCC4. The components of the MMEJ machinery are still largely unknown. Family X DNA polymerases (pols) are involved in the classical NHEJ pathway. We have compared in this work, the ability of human family X DNA pols β, λ and μ, to promote the MMEJ of different model templates with terminal microhomology regions. Our results reveal that DNA pol λ and DNA ligase I are sufficient to promote efficient MMEJ repair of broken DNA ends in vitro, and this in the absence of auxiliary factors. However, DNA pol β, not λ, was more efficient in promoting MMEJ of DNA ends containing the (CAG)n triplet repeat sequence of the human Huntingtin gene, leading to triplet expansion. The checkpoint complex Rad9/Hus1/Rad1 promoted end joining by DNA pol λ on non-repetitive sequences, while it limited triplet expansion by DNA pol β. We propose a possible novel role of DNA pol β in MMEJ, promoting (CAG)n triplet repeats instability.

INTRODUCTION

DNA double-strand breaks (DSBs) repair is accomplished through two main mechanisms: homologous recombination (HR) and non-homologous end joining (NHEJ). Eukaryotic cells possess at least two distinct NHEJ pathways (1). The best known, often referred as the 'classical' NHEJ, relies on the action of a core complex consisting of the Ku70/80 heterodimer and the DNA ligase IV/XRCC4 complex. The second DSBs joining mechanism is Ku- and DNA ligase IV-independent (2), and has been proposed to proceed through microhomology-mediated end joining (MMEJ). The current model proposes that the microhomology regions (5–25 nucleotides) exposed by DNA resection, anneal to form a synaptic complex, generating gaps on both strands, which are filled by a DNA polymerase (pol) and subsequently ligated. Since the resulting DNA junctions are often characterized by deletions, MMEJ is also referred as an error-prone end-joining pathway (3). The components of the MMEJ machinery are still largely unknown. The Mre11-Rad50-Xrs2 complex and the Exo 1 nuclease are required for end processing (4–6), while data from human cells suggested that DNA ligase I is most likely involved in the ligation step of MMEJ (7). In yeast, the translesion DNA pols η, ζ and DNA pol4 have been proposed to participate in MMEJ (8–10). *In Saccharomyces cerevisiae* and *Drosophila melanogaster*, it has been shown an active role of the DNA pol itself in the stabilization of the transient base-pairing interactions occurring at the short microhomology regions in MMEJ. For example, DNA pol4, the only X family pol in *S. cerevisiae*, was found to be absolutely required in end joining, when the gap resulting from the synapsis of two 3′-single strand (ss) DNA overhangs had to be filled using unstable primer–template junctions. Biochemical studies (11) indicated that a unique feature of DNA pol4 in DSBs repair is to stabilize synaptic complexes by bridging the two sides of the broken strands with disrupted base stacking continuity, thus helping to compensate the otherwise unstable DNA duplex at the joint, an activity that perfectly suits to the MMEJ reaction. *D. melanogaster* lacks a DNA pol4 orthologue and biochemical and genetic data suggested that

*To whom correspondence should be addressed. Tel: +39 3825 46354; Fax: +39 3824 22286; Email: maga@igm.cnr.it

mus308/DNA pol θ might be involved in the synthesis step during MMEJ in this organism (12,13).

Mammalian cells possess four X family members: DNA pols λ, β, μ and terminal transferase (TdT) (14). Both DNA pol λ and μ have been shown to have a reduced dependence on stable primer–template pairing and to participate in the 'classical' NHEJ mechanism (15–19). Biochemical studies suggested the existence of a 'gradient' of substrate specificity that dictates the involvement of DNA pols λ and μ in NHEJ, depending on the nature of the broken DNA ends (20). In particular, DNA pol λ preferentially fills gaps with ends that have partially complementary overhangs, while DNA pol μ can catalyze DNA synthesis in the absence of complementarity between the primer and the template strand, and is less active and accurate on DNA ends with complementary overhangs longer than two nucleotides. DNA pol λ, the only family X member conserved through different kingdoms, from plants to prokaryotes to viruses, is the mammalian orthologue of *S. cerevisiae* DNA pol4. Crystal structures of DNA pol λ bound to gapped DNA templates (16,21–24), indicate the presence of specific structural elements (Arg154, Trp274 and Ala510) which take stacking interactions with the template nucleotides at positions 0 and +1, with respect to the primer end, and with the 5′-terminal base of the primer strand gap. Thus, its structural and biochemical features make mammalian DNA pol λ a likely candidate for the synthesis step in MMEJ, which involves unstable primer–template junctions resulting from annealing of 3′-ssDNA overhangs at microhomology regions.

To study the biochemical details of the MMEJ reaction, we have compared in this work, the ability of human family X DNA pols to promote the end joining of different model templates with terminal microhomology regions. Our results reveal specific features of DNA pol λ and β in promoting end joining, depending on the nature of the DNA ends. In particular, with 3′-ss overhangs containing the (CAG)n triplet repeat region of the Huntingtin gene, DNA pol β, but not DNA pol λ, showed a strong tendency to catalyze triplet expansion during MMEJ-dependent DNA synthesis. No human DNA pols have been shown, so far, to have the ability to promote annealing and elongation of 3′-ssDNA overhangs with terminal microhomology regions, in the absence of additional bridging factors. In addition, our data suggest a role of DNA pol β in MMEJ, promoting (CAG)n triplet repeats instability.

MATERIALS AND METHODS

Chemicals

Deoxyribonucleotides were purchased from GeneSpin. Labeled [γ-^{32}P]ATP was purchased from Perkin-Elmer. All other reagents were of analytical grade and purchased from Merck or Fluka. All the oligonucleotides were purchased from Biomers.net (Donau, Germany).

DNA substrates

All oligonucleotides were purified from polyacrylamide denaturing gels (PAGE). Sequences were:

For the MMEJ reaction with non-repetitive sequences:

35-mer:	5′-GAGCATACGGCCAGTGCCGAATTCACACCT**GCGTT**-3′
32-mer:	5′-TATTCGGGAGGTTATATCTTATGAGTC**AACGC**-3′
29-mer:	5′-GGTGTGAATTCGGCACTGGCCGTATGCTC-3′
28-mer:	5′-GTGTGAATTCGGCACTGGCCGTATGCTC-3′
27-mer:	5′-GACTCATAAGATATAACCTCCCGAATA-3′

Annealing of 35-mer with either the 29-mer or 28-mer generated the 29/35 or 28/35-mer donor templates; annealing of the 32-mer with the 27-mer generated the 27/32-mer donor template. End joining with the 27/32 mer in combination with the 29/35 or 28/35-mer templates resulted in the 1 nucleotide (nt)-or 2 nt-gap DNA substrates, respectively. Bold letters highlight the region of terminal microhomology.

For the MMEJ reactions with (CAG)n triplet containing sequences, the oligonucleotides were designed on the basis of the sequence of the human Huntingtin gene (NM_002111.6, nt 179-271):

39-mer:	5′-GAGTCCCTCAAGTCCTTCCAGCAGCAGCAGCAGCA **GCAG**-3′
22-mer:	5′-CGGCGGTGGCGGCTGTTG**CTGC**-3′
28-mer_b:	5′-GCTGCTGCTGGAAGGACTTGAGGGACTC-3′
18-mer_a:	5′-GAAGGACTTGAGGGACTC-3′
18-mer_b:	5′-CAACAGCCGCCACCGCCG-3′

Annealing of the 39-mer with the 28-mer_b or the 18-mer_a resulted in the 28/39-mer or 18/39-mer acceptor templates; annealing of the 22-mer with the 18-mer resulted in the 18/22-mer donor substrate. End joining with the 18/22-mer donor substrate in combination with the 28/39-mer or 18/39-mer acceptor templates resulted in the 7 nt or 17 nt-gap templates, respectively. The CAG repeats on the 39-mer template strand are underlined. Bold letters highlight the region of terminal microhomology.

When indicated, oligonucleotides were 5′-labeled with T4 polynucleotide kinase (NEB) and either unlabeled ATP or [γ-^{32}P]ATP, according to the manufacturer's protocol. Each labeled primer was mixed to the complementary template oligonucleotide at 1:1 (M/M) ratio in the presence of 25 mM Tris–HCl pH 8 and 50 mM KCl, heated at 75°C for 10 min and then slowly cooled down at room temperature.

Proteins

Recombinant human DNA pols λ, β and μ were expressed and purified as described (25,26). Recombinant RP-A and 9-1-1 complexes were expressed and purified as described (27,28).

In vitro polymerase assays

The reaction mixtures contained in a 10 μl final volume: buffer (50 mM Tris–HCl pH 7.5, 1 mM DTT, 0.20 mg/ml

BSA, 2% glycerol), 1 mM $MgCl_2$, DNA substrates, DNA pols, auxiliary proteins and nucleotides in the concentration specified in the Figures. In the end joining reactions, the 'donor' and 'acceptor' templates were added at the beginning of the reaction. All reaction mixtures were incubated for 10 min at 37°C, unless otherwise stated. For denaturing gel analysis of the DNA products, the reaction mixtures were stopped by the addition of standard denaturing gel loading buffer (95% formamide, 10 mM EDTA, xylene cyanol and bromophenol blue), heated at 95°C for 5 min and loaded on a 7 M urea 12% polyacrylamide gel. The reaction products were analyzed by Molecular Dynamics Phosphoimager (Typhoon Trio GE Healthcare) and quantified by Image Quant.

Pull-down experiment

One microgram of purified recombinant his-tagged DNA pol λ wild type, or its truncated mutants N-terminal BRCT/PRD (aa 1–243) or catalytic domain CD (aa 244–575), were incubated with NiNTA agarose beads in PBS 1×. Beads were washed in PBS 1× and added to 1 μg of recombinant purified 9-1-1 complex. Imidazole to a final concentration of 45 mM and NP-40 to a final concentration of 0.1% were added. After incubation for 1 h at 4°C, samples were centrifuged at 600× *g* at 4°C. The supernatant was removed and the beads were washed four times in PBS 1× containing imidazole and NP-40 in the same concentrations as during the binding. Beads were eluted by heating the samples at 100°C in Laemmli sample buffer. After centrifugation at 6000× *g*, the supernatants containing the eluted proteins were loaded onto a 10% SDS–polyacrylamide gel, blotted onto a nitrocellulose membrane and revealed with 9-1-1 specific antibodies.

Kinetic analysis

The variation of the nucleotide incorporation rates (v) as a function of the DNA substrate concentration was fitted to the Briggs–Haldane equation:

$$v = k_{cat}E_0S/(K_d+S) \quad (1)$$

where k_{cat} is the apparent catalytic rate, E_0 is the input enzyme concentration, S is the variable substrate concentration and K_d is the apparent affinity of the enzyme for the substrate.

Where an excess of enzyme over the DNA substrate had to be used, due to the highly distributive nature of the reaction, data were fitted to the modified equation:

$$v = [k_{cat}/(1+K_d/K')E_0S]/\{[K_d/(1+E_i/E_a)]/[(1+K_d/K')+S]\} \quad (2)$$

where k_{cat} is the apparent catalytic rate, E_0 is the input enzyme concentration, S is the variable substrate concentration, K_d is the apparent affinity of the enzyme for the substrate, K' is the equilibrium dissociation constant for the non-productive binding of the enzyme to the substrate, E_i is the fraction of enzyme not involved in catalysis and E_a is the fraction of enzyme involved in catalysis. Fitting was obtained with the GraphPad Prism 3.0 computer program, to estimate the k_{cat} and K_d parameters.

Under distributive synthesis conditions, $k_{cat} = k_{pol}k_{off}/(k_{pol}+k_{off})$ and $K_d = K_sk_{off}/(k_{pol}+k_{off})$, where k_{pol} is the true polymerization rate, k_{off} is the dissociation rate of the enzyme–primer complex and K_s is the true Michelis constant for substrate binding. Thus, the catalytic efficiency k_{cat}/K_d values, correspond to k_{pol}/K_s and were used to compare the efficiency of DNA pols β and λ on the different substrates utilized.

RESULTS

DNA polymerase λ can promote annealing and elongation of DNA strands with limited homology

Two oligonucleotides of, respectively, 32 and 35 nt were designed and their sequences checked to exclude self-annealing and/or hairpin structure formation. These two oligonucleotides possessed a five nucleotides complementary region at their 3′-ends. Thus, upon annealing they generate a structure (Figure 1a, top) where the 3′-OH end of each strand provides the primer to copy the other strand. The calculated temperature (Tm) of the two annealed oligonucleotides under these conditions was 16°C, while all reactions were carried out at 37°C, ensuring that spontaneous annealing did not occur. Since the sequences of each strand were different, appropriate combinations of dNTPs could be used to selectively start synthesis on one strand or the other. Synthesis was monitored by radioactively labeling the 5′-end of one strand. DNA pol λ was incubated first with the 5′-labeled 32-mer alone (Figure 1a, lanes 1–5). In agreement with our previous observations (28), DNA pol λ showed limited template-independent terminal transferase (tdt)-like activity, being able to incorporate dATP (lane 1) and, to a very limited extent, dTTP (lane 4). Synthesis was always limited to 1–2 nucleotides, even in the presence of all four dNTPs (lane 5). Conversely, when the unlabeled partially complementary 35-mer was added to the reaction together with the 5′-labeled 32-mer (Figure 1a, lanes 6–10), addition of all four dNTPs resulted in the appearance of elongated products (lane 10 marked by an asterisk). Addition of dATP and dGTP (lane 11), or dATP, dGTP and dTTP (lane 12), under these conditions, resulted in the synthesis of the products expected from the sequence of the 35-mer template strand. Similarly, when the label was on the 35-mer strand, (Supplementary Figure 1a), nucleotide incorporation was dictated by the sequence of the complementary 32-mer strand. These results suggested that DNA pol λ was able to promote annealing and template-dependent elongation of 3′-ssDNA strands with terminal microhomology.

DNA polymerase λ requires terminal microhomology to promote strand annealing and elongation

Next the 5′-labeled 32-mer primer strand was used in combination with its partially complementary 35-mer, or a non-complementary 29-mer, in the presence of both dATP and dGTP, which should allow synthesis of a +3 product on both template strands (Figure 1b, top scheme). DNA pol λ catalyzed the formation of the

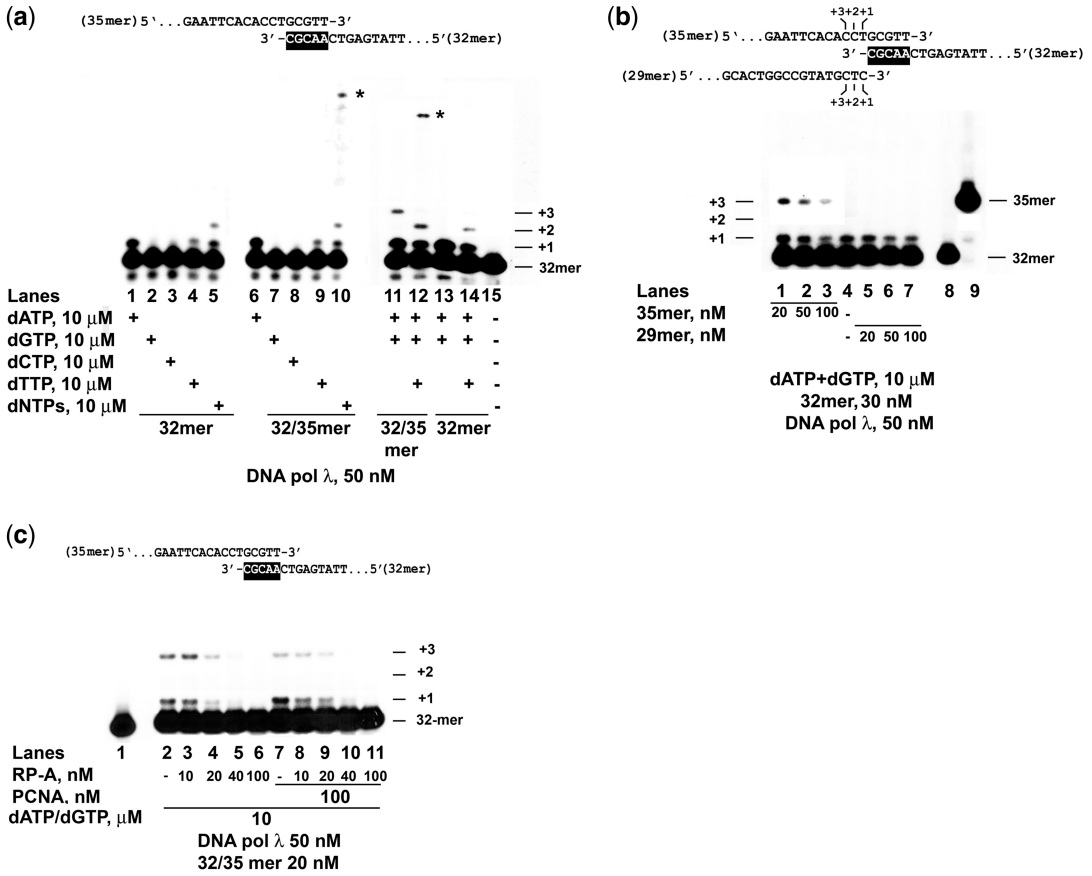

Figure 1. DNA polymerase λ can promote annealing and elongation of DNA strands with limited homology. (**a**) DNA pol λ was incubated with 30 nM of the 5′-labeled 32-mer alone (lanes 1–5,13,14) or in combination with its partially complementary 35-mer (lanes 6–12) and various nucleotide combinations. Lane 15: control reaction in the absence of DNA pol λ. (**b**) DNA pol λ was incubated with 30 nM of the 5′-labeled 32-mer in combination with its partially complementary 35-mer (lanes 1–3) or with a non-complementary 29-mer (lanes 5–7). Lane 4: reaction with 32-mer alone. Lane 8, 9: labeled 32-mer and 35-mer oligonucleotides loaded as markers. (**c**) DNA pol λ was incubated with 20 nM of the 5′-labeled 32-mer in combination with its partially complementary 35-mer, in the absence (lanes 2, 7) or in the presence of RP-A alone (lanes 3–6) or together with PCNA (lanes 8–11). Lane 1: control reaction in the absence of DNA pol λ.

expected elongation products only in the presence of the partially complementary 35-mer template strand (Figure 1c, lanes 1–3), whereas, in the presence of the labeled 32-mer strand alone or together with the non-complementary 29-mer, the incorporation was limited to one nucleotide (lanes 4–7), due to the tdt-like activity of DNA pol λ. Molar excess of ss 35-mer inhibited the reaction, likely due to sequestration of the enzyme. Analysis of the dependence of nucleotide incorporation from the 35-mer template strand concentrations, allowed the determination of an apparent affinity (K_d) of DNA pol λ for the template of 170 nM and a catalytic efficiency (k_{cat}/K_d) of 0.3 $\mu M^{-1}min^{-1}$ (Table 1). In comparison, the corresponding values of DNA pol λ for a standard primer/template junction were 43 nM and 5.4 $\mu M^{-1}min^{-1}$ (26).

Effect of replication protein A and proliferating cell nuclear antigen on the ability of DNA polymerase λ to promote strand annealing and elongation

The single-stranded DNA-binding protein RP-A and the auxiliary factor PCNA, have been shown to influence the ability of DNA pol λ to bind and elongate a DNA primer (28), thus we asked whether these two proteins were able to affect the ability of DNA pol λ to catalyze the MMEJ reaction. In the presence of the 5′-labeled 32-mer primer strand and its partially complementary 35-mer, RP-A reduced the synthesis by DNA pol λ (Figure 1c, lanes 2–6), also in the presence of its auxiliary factor PCNA (lanes 7–11), likely due to sequestration of the ssDNA, which prevented annealing of the complementary regions. These data indicated that the presence of ssDNA with terminal microhomology regions between the two strands was essential for the ability of DNA pol λ to promote their annealing and subsequent template-dependent elongation.

DNA polymerase λ requires a 5′-phosphate for the annealing of short 3′-single strand DNA overhang and subsequent gap filling, generating ligatable nicks

Next, two 'acceptor' templates, A and B, with, respectively, a 6 or 7 nt 3′-ss overhang and a 'donor' primer with a 5 nt 3′-ss overhang, complementary to the last 5 nt of the acceptor strands, were used (Figure 2a). Upon annealing of the 'acceptor' and 'donor' templates

Table 1. Kinetic parameters for MMEJ-dependent template binding and elongation by DNA polymerase λ on different DNA substrates

Substrate[a]	Acceptor template	Donor primer	K_d (μM)[b]	k_{cat} (min^{-1})	k_{cat}/K_d ($\mu M^{-1}min^{-1}$)
ss 35-mer	ss 35-mer	ss 32-mer	0.17 ± 0.01	0.05 ± 0.01	0.3
1 nt gap unphosphorylated	29/35-mer	27/32-mer	1.08 ± 0.2	0.012 ± 0.003	0.011
phosphorylated	29/35-mer	27/32-mer	0.15 ± 0.02	0.12 ± 0.02	0.8
ss 39-mer $(CAG)_6$	39-mer	ss 22-mer	0.15 ± 0.02	0.041 ± 0.003	0.27
17 nt gap $(CAG)_6$ phosphorylated	18/39-mer		0.12 ± 0.02	0.015 ± 0.005	0.125
7 nt gap $(CAG)_3$ phosphorylated	28/39mer		0.5 ± 0.1	0.007 ± 0.001	0.014

[a]The sequence of the different oligonucleotides used is given in 'Materials and Methods' section. The structure of the different substrates is indicated in the Figures.
[b]The kinetic parameters K_d, k_{cat} and k_{cat}/K_d were calculated as indicated in the 'Material and Methods' section. Values are the means of three independent experiments ± S.D.

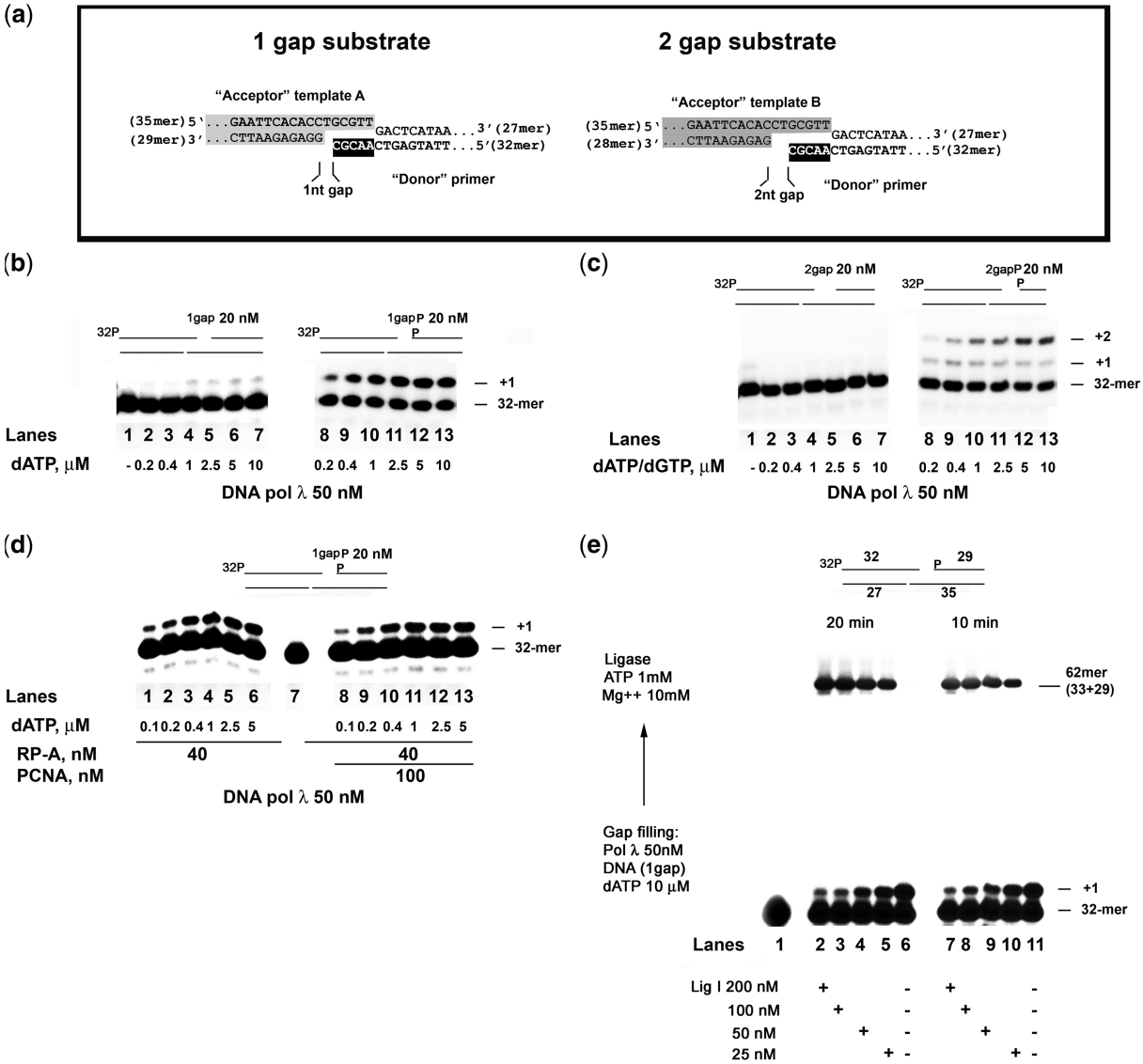

Figure 2. DNA polymerase λ requires a 5′-phosphate for annealing of short 3′-single stranded DNA overhangs and subsequent gap filling thus generating ligatable nicks. (**a**) Schematic diagram of the oligonucleotide pairs used to generate the 1 nt- and 2 nt-gap substrates. The 32-mer strand was radioactively 5′-labeled in all cases. Black boxes indicate the region of microhomology between the 3′-ss overhangs. (**b**) DNA pol λ was incubated with the 1 nt-gap template unphosphorylated (lanes 1–7) or bearing a 5′-phosphorylated end downstream of the gap (lanes 8–13), in the presence of increasing amounts of dATP. (**c**) DNA pol λ was incubated with the 2 nt-gap template unphosphorylated (lanes 1–7) or bearing a 5′-phosphorylated end downstream of the gap (lanes 8–13), in the presence of increasing amounts of dATP and dGTP. (**d**) DNA pol λ was incubated with the 1 nt-gap template bearing a 5′-phosphorylated end downstream of the gap in the presence of increasing amounts of dATP and in the presence of RP-A alone (lanes 1–6) or together with PCNA (lanes 8–13). Lane 7: labeled 32-mer was loaded as a marker. (**e**) DNA pol λ was incubated with 50 nM of the 1 nt-gap template bearing a 5′-phosphorylated end downstream of the gap and dATP. Increasing amounts of DNA ligase I was added and ligation incubated for 20 min (lanes 2–5) or 10 min (lanes 7–10). Lanes 6, 11: the gap-filling reactions stopped before the addition of DNA ligase I. Lane 1: labeled 32-mer was loaded as a marker.

at the region of terminal microhomology, two different substrates, mimicking the structure generated by DNA DSBs, were generated with a 1 nt- or 2 nt-gap (Figure 2a). The calculated Tm for the annealing of these templates at the microhomology regions, under these conditions, was 16°C, ensuring no spontaneous self-annealing at the temperature of 37°C, used in all reactions. DNA pol λ showed a 40-fold increase in its catalytic activity on the 1 nt-gapped template, when the 5′-recessed end of the 29/35-mer acceptor template A was phosphorylated (Figure 2b, compare lanes 2–7 with lanes 8–13; Table 1). Such a phosphorylated 5′-end was even absolutely required for DNA pol λ activity on the 2 nt-gapped substrate (Figure 2c, compare lanes 2–7 with lanes 8–13). Kinetic analysis showed that DNA pol λ utilized the 5′-phosphorylated 1 nt-gap substrate with a 2-fold higher catalytic efficiency than the ss 35-mer template (Table 1). Contrary to what previously observed (Figure 1c), RP-A did not prevent the microhomology-mediated gap-filling synthesis by DNA pol λ on the 1 nt-gap (Figure 2d) or 2 nt-gap (Supplementary Figure S1e) substrates. As shown in Figure 2e, in the presence of DNA ligase I, the +1 products resulting from gap filling by DNA pol λ on the 1 nt-gap substrate, were converted into fully ligated products in a dose- and time-dependent manner (lanes 2–11). These results indicated that DNA pol λ and DNA ligase I were sufficient to promote efficient repair of broken DNA ends with terminal microhomologies.

The alternative clamp Rad9/Hus1/Rad1 (9-1-1) complex enhances the processivity of DNA polymerase λ during microhomology-mediated end joining by physical interaction with its catalytic domain

The 9-1-1 complex is an important component of the cellular response to DNA DSBs (29). When added to the reaction, it stimulated the MMEJ reaction catalyzed by DNA pol λ on the 5′-labeled ss 32-mer together with the ss 35-mer template (Figure 3a, lanes 2–5) and on the 1 nt-gap substrate (lanes 7–10). When DNA pol λ was tested on the 5′-labeled ss 32-mer together with the ss 35-mer template and all four dNTPs, 9-1-1 stimulated DNA synthesis (Figure 3b, compare lanes 9, 10 with lanes 19, 20). The stimulation of DNA pol λ by 9-1-1 could be due either to an increased ability of DNA pol λ to promote the strand annealing at the microhomology region, or to an increase in its DNA synthetic activity. To further investigate the effect of 9-1-1 on the end joining-dependent synthetic activity, the experiments were then repeated in the absence or presence of a molar excess of unlabeled trap ssDNA. Addition of the unlabeled trapping DNA at different incubation times, will cause any enzyme molecule dissociating from the template to be sequestered, thus effectively preventing multiple turnovers. Thus, comparison of the products synthesized as a function of the trap addition time, with the products synthesized in the absence of trap and in the presence or in the absence of 9-1-1, allowed to evaluate any effect of 9-1-1 on the processivity of DNA pol λ. Comparison of the products synthesized as a function of the trap addition time, with the products synthesized in its absence, revealed that full-length products were visible at earlier time points after trap addition in the presence of 9-1-1 (lanes 3, 4), than in its absence (lanes 12, 13). As already shown above (Figure 1c), RP-A inhibited DNA synthesis by DNA pol λ on the partially complementary 32-mer and 35-mer ssDNA substrates. Interestingly, addition of the 9-1-1 complex was able to counteract this inhibition by RP-A (Figure 3c, compare lane 2 with lanes 3–5). Finally, a pull-down experiment with recombinant proteins, revealed a physical interaction of 9-1-1 with the C-terminal catalytic domain (aa 244–575) of DNA pol λ (Figure 3d, lanes 4 and 5), suggesting that 9-1-1 increased the processivity of DNA pol λ in the MMEJ reaction through protein–protein interaction with the pol catalytic domain.

DNA polymerase λ catalyzes aberrant end joining products, starting from 3′-single stranded DNA overhangs containing CAG triplet repeats

The MMEJ repair of broken DNA strands might also be important in the context of DSBs repair of regions containing repetitive sequences. We next exploited in MMEJ, the sequence of the 5′-end of the human Huntingtin gene, known to contain several CAG triplet repeats. Two oligonucleotide pairs, derived from the Huntingtin gene, were employed (Figure 4a): a 18/39-mer 'acceptor' template, with a 21 nt ss 3′-overhang, consisting of seven consecutive CAG repeats and a 18/22-mer 'donor' primer, with a 4 nt ss 3′-overhang (CTGC), complementary to the last four nucleotides of the ss 3′-overhang of the 18/39-mer. Upon annealing, a double-stranded DNA with a 17 nt gap, bearing CAG repeats on the template strand, is generated (Figure 4a). Gap-filling DNA synthesis starting from the 3′-OH end of the 22-mer strand, will give a 39 nt product (17 nt newly synthesized + 22 nt from the annealed primer strand). DNA pol λ showed no incorporation in the presence of the 18/22-mer 'donor' labeled on the 5′-end of the 22-mer strand, either alone or in combination with the 18/39-mer 'acceptor' template (Figure 4b). Surprisingly, in the presence of the 18/39-mer 'acceptor' labeled on the 5′-end of the 39-mer strand, either alone, or in combination with the complementary unlabeled 18/22-mer 'donor' substrate, DNA pol λ catalyzed the synthesis of long products (Figure 4c). The synthesis on this substrate was inefficient, requiring high DNA pol λ concentrations. In the presence of the labeled 18/39-mer alone, addition of dCTP (Figure 4d, lane 1), or dCTPand dTTP (Figure 4d, lane 5), resulted in the synthesis of +1 and +2 products, respectively, as expected if the 39-mer strand was used as the template to be copied. This suggested that DNA pol λ promoted self annealing of the ssDNA 3′ overhangs of two 18/39-mer molecules into a head-to-head fashion, using the homology regions between the repetitive sequences (Figure 4e). The resulting DNA structures are more stable (Tm 12°C–26°C) than the 17 nt-gap substrate resulting from the annealing of the 4 nt 3′-overhang of the 18/22-mer 'donor' to its complementary sequence on the 39-mer strand (Tm below 12°C). Accordingly, when a molar excess of the 22/18-mer

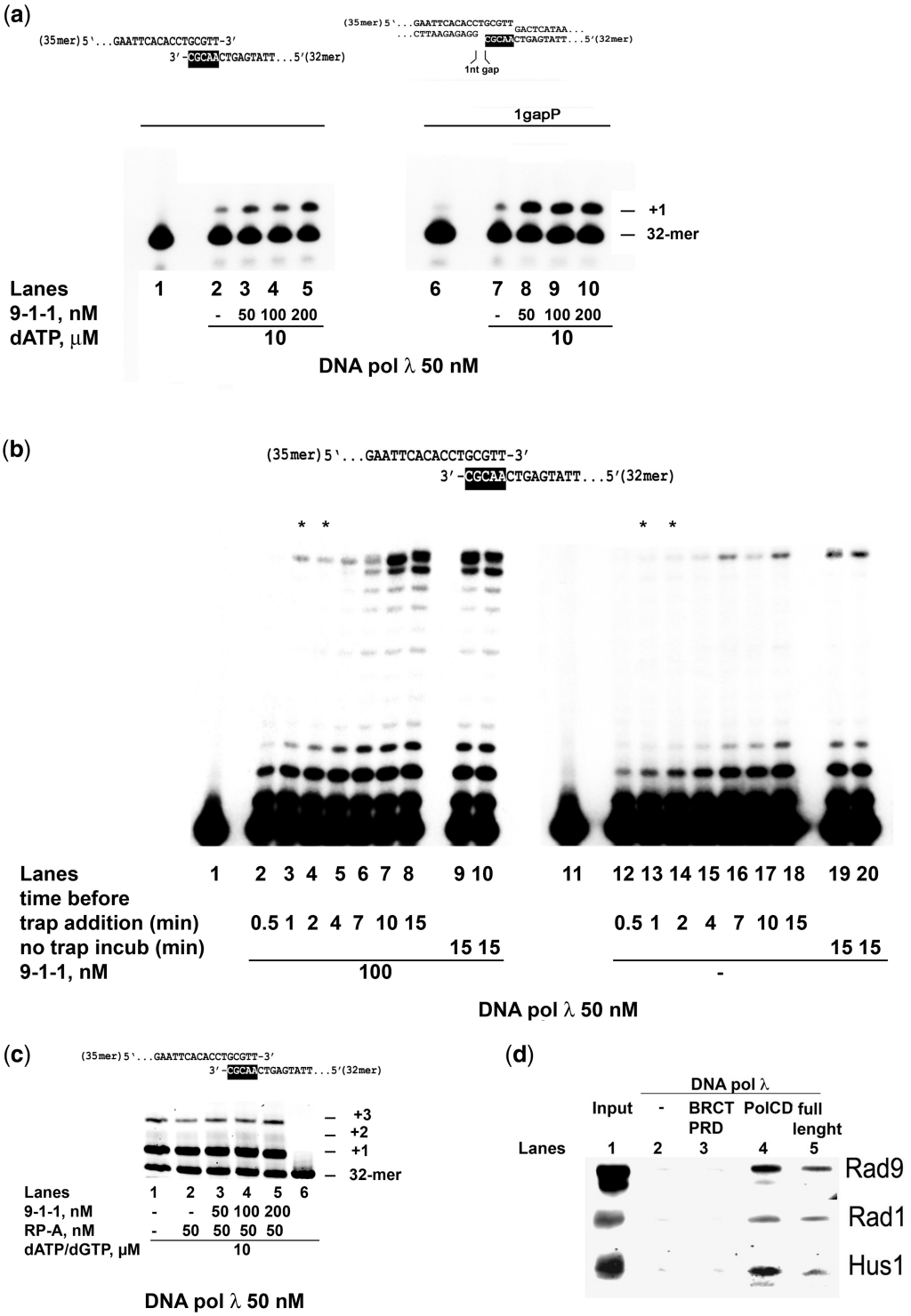

Figure 3. The Rad9/Hus1/Rad1 (9-1-1) complex functionally and physically interacts with DNA polymerase λ during microhomolgy-mediated end joining. (**a**) DNA pol λ was incubated with 50 nM of the 5′-labeled 32-mer in combination with its partially complementary 35-mer (lanes 2–5) or with 50 nM of the 1 nt-gap template bearing a 5′-phosphorylated end downstream of the gap (lanes 7–10), in the absence (lanes 2, 7) or in the presence of increasing amounts of 9-1-1. Lanes 1, 6: control reactions in the absence of DNA pol λ. (**b**) DNA pol λ was incubated with 50 nM of the 5′-labeled 32-mer in combination with its partially complementary 35-mer in the presence (lanes 2–10) or in the absence (lanes 12–20) of 9-1-1, for 15 min (lanes 9, 10 and 19, 20). At different time points during the incubation, excess (1 μM) of unlabeled DNA trap was added (lanes 2–8 and 12–18) and incubation continued up to 15 min. Asterisks mark the earliest time points of trap addition when full length products were detected. (**c**) DNA pol λ was incubated with 50 nM of the 5′-labeled 32-mer in combination with its partially complementary 35-mer in the absence (lane 1), or in the presence (lanes 2–5) of RP-A and in the absence (lanes 1, 2) or in the presence (lanes 3–5) of increasing amounts of 9-1-1. Lane 6: control reaction in the absence of DNA pol λ (**d**) Recombinant 9-1-1 (lane 1) was incubated in the absence (lane 2) or in the presence of his-tagged DNA pol λ full length (lane 5) or its truncated mutants BRCT/PRD (aa 1–243; lane 3) or catalytic domain (CD, aa 244–575; lane 4). Pulled-down proteins were separated by SDS–PAGE, blotted and analyzed with 9-1-1 specific antibodies.

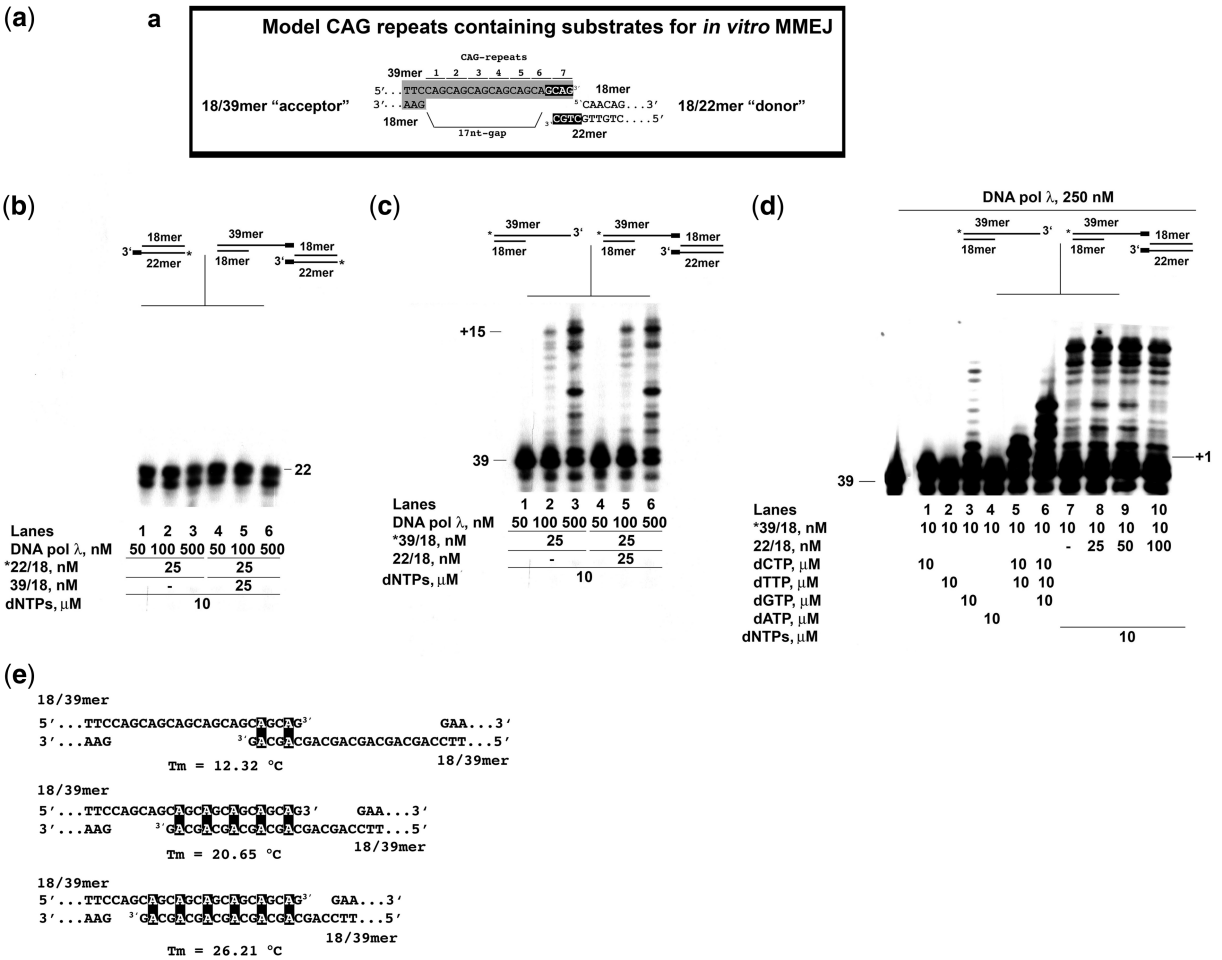

Figure 4. DNA polymerase λ catalyzes aberrant end joining products with 3′-single-stranded DNA overhangs containing triplet repeats. (**a**) Schematic diagram of the two oligonucleotide pairs used to generate the 17 nt-gap substrate. The seven triplet repeats present on the 'acceptor' template strand are numbered on top of the strand. The black box shows the terminal microhomology region. (**b**) DNA pol λ was titrated with the 18/22-mer 'donor' template alone (lanes 1–3) or in combination with the 39/18-mer 'acceptor' template (lanes 4–6), in the presence of 10 μM dNTPs. The 22-mer strand was 5′ labeled in all the lanes. (**c**) DNA pol λ was titrated with the 39/18-mer 'acceptor' template alone (lanes 1–3) or in combination with the 18/22-mer 'donor' template (lanes 4–6), in the presence of 10 μM dNTPs. The 39-mer strand was 5′ labeled in all the lanes. (**d**) DNA pol λ was incubated with the 18/39-mer substrate, 5′-labeled on the 39-mer strand alone with different nucleotide combinations (lanes 1–7), or in the presence of 10 μM dNTPs and increasing amounts of the unlabeled 18/22-mer substrate (lanes 8–10). (**e**) Schematic diagram of representative possible structures resulting from head-to-head annealing of the 3′-ss overhangs of two 18/39-mer templates. Black boxes indicate the mismatches. Theoretical melting temperatures (Tm), calculated under the reaction conditions used in the assays, are indicated below each structure.

'donor' template was added to the reaction, in the presence of the labeled 18/39-mer, no reduction in the synthesized products starting from the 39-mer labeled strand was observed (Figure 4d, lanes 7–10), indicating that the 18/22-mer was unable to compete with the 39-mer strand for annealing to the complementary sequence. These results suggested that DNA pol λ more efficiently promoted the formation of aberrant head-to-head 18/39-mer dimers, instead of properly annealing the 18/39-mer 'acceptor' to the 18/22-mer 'donor' substrate.

DNA polymerases β and μ show different properties in the annealing and template-dependent elongation of single-strand 3′-DNA overhangs

As shown in Supplementary Figure S1b, contrary to DNA pol λ, DNA pol β showed no incorporation in the presence of the partially complementary 32-mer and 35-mer oligonucleotides, while on a standard template/primer substrate, DNA pols β and λ showed similar activities (Supplementary Figure S1c). DNA pol μ under similar conditions (Supplementary Figure S1d) showed template-independent tdt-like activity, as already reported (25). Either in the presence of the labeled ss 32-mer alone or in combination with the partially complementary 35-mer, the best incorporated nucleotide was dCTP (lanes 3, 8) and addition of all four dNTPs resulted in a pattern identical to the one observed with dCTP alone (compare lanes 5, 10 with lanes 3, 8). These data suggested that the ability to promote annealing and elongation of partially complementary ssDNA strands is a property of DNA pol λ but not of DNA pols β and μ. Interestingly, in the presence of the 5′-phosphorylated 1 nt-gap substrate, DNA pol β was able to promote

annealing and elongation, albeit with lower efficiency than DNA pol λ (Supplementary Figure S1f, compare lanes 1–5 with lanes 6–11), suggesting that the structure of the DNA ends to be joined (fully ss or partially ds with 3′-ss overhangs) might influence the ability of DNA pol β to perform the MMEJ reaction. Thus, DNA pol β was further investigated in the context of MMEJ of CAG repeats-containing DNA ends.

DNA polymerase β promotes CAG triplet expansion during microhomology-mediated end joining of DNA ends bearing repetitive sequences

DNA pol β was tested in the MMEJ *in vitro* system, using the 18/22-mer oligonucleotide pair as the 'donor' substrate, in combination with three different 'acceptor' substrates (Figure 5a): the 39-mer alone, the 18/39-mer and an additional 28/39-mer template, with a 11 nt ssDNA 3′-overhang, bearing only three CAG repeats. Annealing of the terminal 4 nt of this overhang to its complementary strand on the 18/22-mer 'donor' substrate, would generate a 7 nt gap, containing two CAG repeats (Figure 5a). Titration of the ss 39-mer 'acceptor' substrate, in the presence of a fixed concentration of the 18/22-mer 'donor', labeled at the 5′-end of the 22-mer strand, showed a dose dependent increase in the nucleotide incorporation by DNA pol β, albeit only at high enzyme concentrations (Figure 5b, lanes 1–4). The same experiment in the presence of the 18/39-mer 'acceptor' substrate, showed accumulation of the 39 nt product, resulting from complete filling of the 17 nt gap, along with longer products (Figure 5b, lanes 5–8). When the 28/39-mer 'acceptor' template was tested in combination with the labeled 22/18-mer 'donor', resulting in the 7 nt-gap substrate (Figure 5a scheme), DNA pol β catalyzed the synthesis of a 29 nt product, as expected from complete filling of the 7 nt gap, plus additional longer products (Figure 5c, lanes 3–8). Comparison with an oligonucleotide size marker ladder (lane 2) showed that these products were evenly spaced, each being 3 nt apart. At least 10 additional trinucleotide repeats were added to the 29 nt full-length product. Even assuming strand displacement by DNA pol β, the number of available additional triplets to be copied could not exceed three to four (Figure 5a scheme). Thus, these products are indicative of triplet expansions. As documented in Table 2, DNA pol β utilized all three 'acceptor' substrates with similar efficiencies, with a 2-fold preference for the 28/39-mer. Synthesis by DNA pol β on the 28/39-mer substrate was strictly template-dependent, with the expected +1 product appearing only in the presence of the first encoded nucleotide dTTP (Supplementary Figure S2a) according to the sequence of the 39-mer template strand. When DNA pol λ was tested with the 28/39-mer 'acceptor' in combination with the labeled 18/22-mer 'donor', no synthesis was detected (Supplementary Figure S2b). Thus, DNA pol β and DNA pol λ appear to have different specificities for MMEJ on normal or repetitive sequences.

The ability of DNA polymerases β and λ to promote microhomology-mediated end joining is influenced by the structure of the DNA ends

Next, the activity of DNA pols λ and β was compared, in the presence of the three different 'acceptor' substrates (39-mer, 18/39-mer and 28/39-mer), but with the 5′-labeled 22-mer ss oligonucleotide as 'donor' (Figure 5d). As shown in Figure 5e, DNA pol λ was able to start DNA synthesis from the ss 22-mer. A strong accumulation of short (+1 to +2) products could be observed (lanes 1–9) with all 'acceptor' substrates. A similar pattern was observed in the presence of the labeled 22-mer strand alone (lanes 20, 21), suggesting that those products were due to the template-independent elongation of the ss 22-mer by the tdt-like activity of DNA pol λ. In the presence of the 'acceptor' substrates synthesis of longer products was also detected. However, this synthesis decreased with the shortening of the 3′-ss overhang of the 'donor' substrate, from 39 nt (39-mer, lanes 1–3) to 21 nt (18/39-mer, lanes 4–6), almost disappearing at 11 nt (28/39-mer, lanes 7–9). DNA pol β was also able to start DNA synthesis from the ss 22-mer 'donor' oligonucleotide. Similarly to DNA pol λ, the efficiency of DNA pol β decreased as the length of the ssDNA 3′-overhang was reduced (lanes 10–18). Kinetic analysis showed that DNA pol β utilized the ss 22-mer 'donor' less efficiently than the 18/22-mer, on all the 'acceptor' templates (Table 2). Comparison of the k_{cat}/K_d values of DNA pol λ (Table 1) and DNA pol β (Table 2) on these substrates, revealed that DNA pol λ showed a preference for the ss 22-mer 'donor' in combination with the ss 39-mer 'acceptor' template, while DNA pol β more efficiently utilized the ss 22-mer 'donor' in combination with the 18/39-mer 'acceptor'. Thus, the efficiency of MMEJ of DNA ends containing CAG triplet repeats by DNA pols β and λ was influenced by the nature of the 'donor' strand (either partially ds or ss) and the length of the 3′- ss overhang of the 'acceptor' strand.

The Rad9/Hus1/Rad1 (9-1-1) complex might reduce triplet expansion by DNA polymerase β

DNA pol β promoted significant triplet expansion during MMEJ of DNA ends containing CAG triplet repeats (Figure 5). RP-A did not affect the size or distribution of the products generated by DNA pol β starting from the 18/22-mer 'donor' with all the acceptor substrates: 39-mer (Figure 6a, lanes 1–4); 18/39-mer (lanes 5–8); 28/39-mer (lanes 9–12). The 9-1-1 complex functionally and physically interacted with DNA pol λ in the MMEJ reaction (Figure 3). However, 9-1-1 was unable to promote synthesis by DNA pol λ on the triplet repeats 28/39-mer 'acceptor' substrate, in the presence of the 18/22-mer donor (Figure 6b, lanes 1–4). Since the 9-1-1 complex has been shown to physically interact with DNA pol β (27), we tested its effect on DNA pol β with the 18/22-mer 'donor' and the 28/39-mer 'acceptor' substrates. The 9-1-1 complex inhibited DNA pol β (Figure 6b, lanes 5–8). However, as reported in Figure 6c, the 29 nt product, representing precise gap filling without triplet expansion, was less inhibited than longer triplet expansion

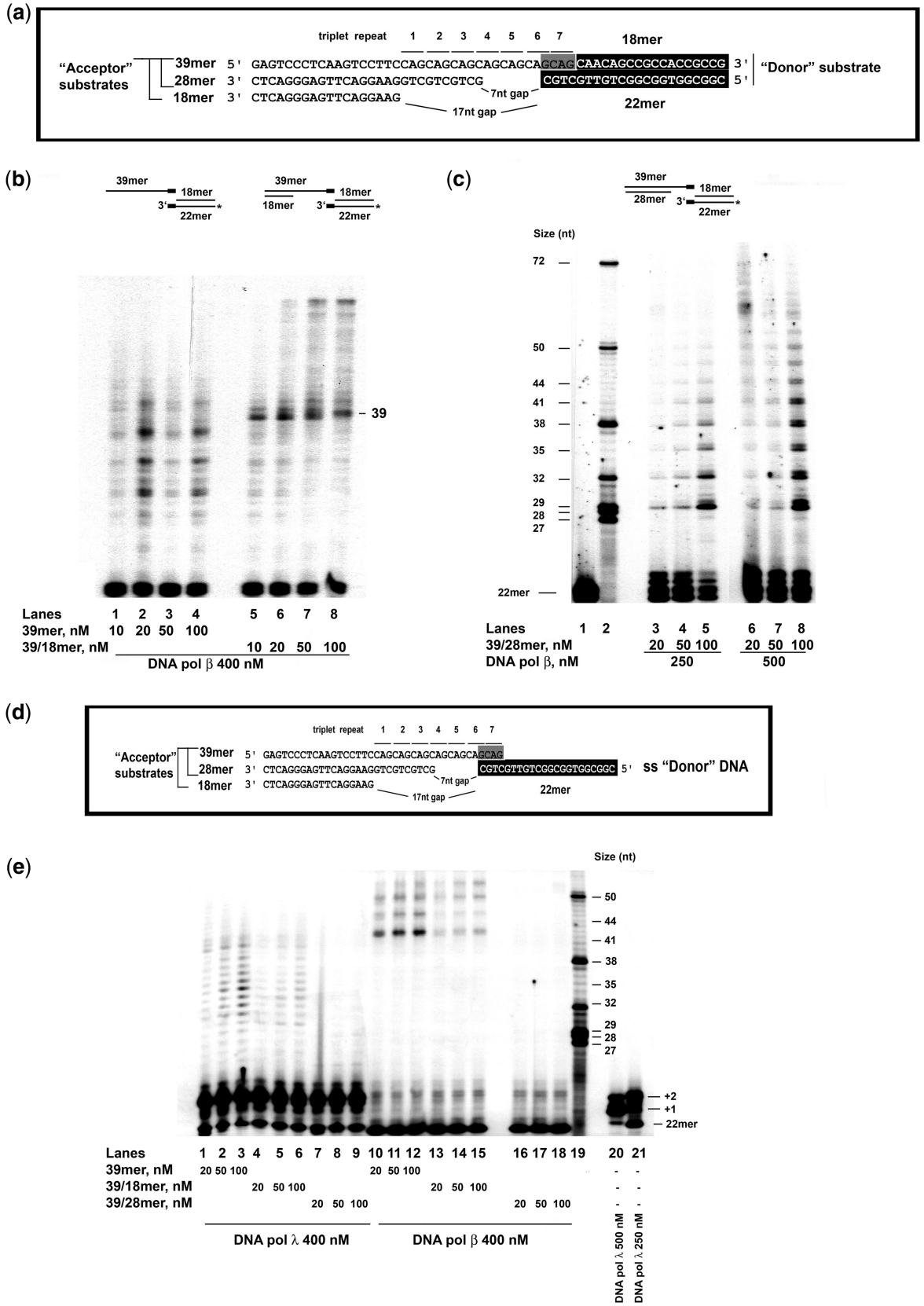

Figure 5. DNA polymerase β promotes CAG triplet expansion during microhomology-mediated end joining. (**a**) Schematic diagram of the different oligonucleotide pairs used to generate the different substrates. The common 18/22-mer 'donor' substrate is shaded in black. The grey box identifies the terminal microhomology sequence on the 3′-ss overhang common to all the 'acceptor' substrates. The size of the gaps resulting from microhomology-mediated annealing of the terminal nucleotides is indicated. The seven CAG triplet repeats present on the 'acceptor' template strand are numbered on top of the strand. (**b**) DNA pol β was incubated in the presence of 10 μM dNTPs and 50 nM of the 18/22-mer 'donor'

(continued)

Table 2. Kinetic parameters for MMEJ-dependent template binding and elongation by DNA polymerase β on CAG triplets-containing substrates, with the 18/22-mer or ss 22-mer 'donor' primers

Substrate[a]	Acceptor template	Donor primer	K_d (μM)[b]	k_{cat} (min^{-1})	k_{cat}/K_d ($\mu M^{-1}min^{-1}$)
ss 39-mer $(CAG)_6$	39-mer	18/22-mer	0.031 ± 0.003	0.03 ± 0.01	0.96
17 nt gap $(CAG)_6$ phosphorylated	18/39-mer		0.029 ± 0.002	0.05 ± 0.02	1.7
7 nt gap $(CAG)_3$ phosphorylated	28/39-mer		0.035 ± 0.005	0.08 ± 0.01	2.3
ss 39-mer $(CAG)_6$	39-mer	ss 22-mer	0.12 ± 0.02	0.045 ± 0.005	0.37
17 nt gap $(CAG)_6$ phosphorylated	18/39-mer		0.14 ± 0.02	0.09 ± 0.01	0.64
7 nt gap $(CAG)_3$ phosphorylated	28/39-mer		0.1 ± 0.02	0.004 ± 0.001	0.04

[a]The sequence of the different oligonucleotides used is given in 'Materials and Methods' section. The structure of the different substrates is indicated in the Figures.
[b]The kinetic parameters K_d, k_{cat} and k_{cat}/K_d were calculated as indicated in the 'Material and Methods' section. Values are the means of three independent experiments ± S.D.

products, suggesting that 9-1-1 might reduce CAG triplet expansion by DNA pol β during MMEJ.

DISCUSSION

A role for DNA polymerase λ and the 9-1-1 complex in MMEJ

The family X DNA pols λ and μ are considered to play non-overlapping roles in NHEJ, depending on the nature of the broken DNA ends (20). DNA pol λ is more efficient with ends that have partially complementary overhangs, while DNA pol μ can catalyze DNA synthesis in the absence of complementarity. Here, we provide evidence for a possible role of DNA pol λ in the alternative end-joining pathway MMEJ. DNA pol λ is able to promote the annealing of ssDNA 3′-overhangs at regions of homology as short as five nucleotides and uses the resulting primer/template structures for elongation. Based on these observations, we propose the following model for DNA pol λ-dependent MMEJ (Figure 6d). Broken DNA ends normally undergo resection in a 5′ → 3′ direction, generating ss 3′-DNA overhangs. In the presence of short complementary regions between the two strands, DNA pol λ can efficiently bind and stabilize their junctions, starting DNA synthesis from the 3′-OH ends. The length of the 5′ ssDNA-template overhang is important for the stability of the synaptic complex. DNA pol λ can efficiently promote pairing of ss 3′-DNA overhangs at micro-homology region, whose joining results in long (30 nt) ss-template overhangs. However, with short (6 nt) ss 3′-overhangs, whose junction results in a 1 nt- or 2 nt-gapped template, DNA pol λ requires a 5′-phosphate to be present at the ds region on the 5′ side of the gap (Figure 2d, c; Table 1). This is in agreement with the known high affinity of the 8 kDa dRPlyase domain of DNA pol λ for the downstream 5′ phosphate on gapped templates (21,22). Thus, when DNA pol λ approaches to the end, stable binding is ensured by the presence of the 5′ phosphate on the downstream double-stranded part, allowing precise gap filling, which results in a nick suitable to be sealed by DNA Ligase I. In this context, the fact that the processivity of DNA pol λ is enhanced through physical interaction with the 9-1-1 complex might be physiologically relevant. The 9-1-1 heterotrimer is an important component of the DNA damage response pathway and interacts with several BER proteins, including DNA pol β, stimulating their activity (27,30–32) and has been linked to the repair of DSBs (29,33). Thus, in this minimal *in vitro* system, DNA pol λ and DNA ligase I, in the absence of additional stabilizing factors, appear capable to carry out MMEJ of broken DNA ends with terminal microhomologies.

Different substrate specificities of DNA polymerases λ and β during MMEJ of broken DNA ends with terminal repetitive DNA sequences

When a break occurs within a DNA region rich in repetitive sequences, the resulting ends will show extensive homology to each other, thus constituting an ideal substrate for the MMEJ pathway. In this context, the structure of the ends to be joined appears to be critical for DNA pol λ. In fact, when supplemented with two DNA ends, one terminating with a long 3′ ssDNA-overhang (7–39 nt) containing several CAG triplet repeats, and the other one bearing a short (4 nt) 3′ ssDNA-overhang with a single GTC repeat on the complementary strand, DNA pol λ invariably promoted the

Figure 5. Continued
template, 5′ labeled on the 22-mer strand, in combination with increasing amounts of the 39-mer ss (lanes 1–4), or the 39/18-mer (lanes 5–8) 'acceptor' templates. (**c**) DNA pol β at 250 nM (Lanes 3–5) or 500 nM (lanes 6–8), was incubated in the presence of 50 nM of the 18/22-mer 'donor' template, 5′ labeled on the 22-mer strand, in combination with increasing amounts of the 39/28-mer 'acceptor' template and 10 μM dNTPs. Lane 1: control reaction in the absence of nucleotides. Lane 2: oligonucleotide size marker ladder. (**d**) The sequences of the different oligonucleotide pairs used are shown on top of the panel. The common 22-mer ss 'donor' oligonucleotide substrate is shaded in black. The grey box identifies the terminal microhomology sequence on the 3′-overhang part common to both the 'acceptor' substrates. The size of the gaps resulting from microhomology-mediated annealing of the terminal nucleotides is indicated. DNA pol λ (lanes 1–9) or DNA pol β (lanes 10–18) were incubated in the presence of the 5′-labeled 22-mer ss 'donor' oligonucleotide substrate and with increasing concentrations of the 39-mer ss 'acceptor' oligonucleotide (lanes 1–3 and 10–12), or the 39/18 (lanes 4–6 and 13–15) or 39/28 (lanes 7–9 and 16–18) acceptor templates. Lane 19: oligonucleotide size marker ladder. Lanes 20, 21: 5′-labeled 22-mer ss oligonucleotide incubated in the presence of 10 μM dNTPs and 250 nM or 500 nM DNA pol λ, respectively.

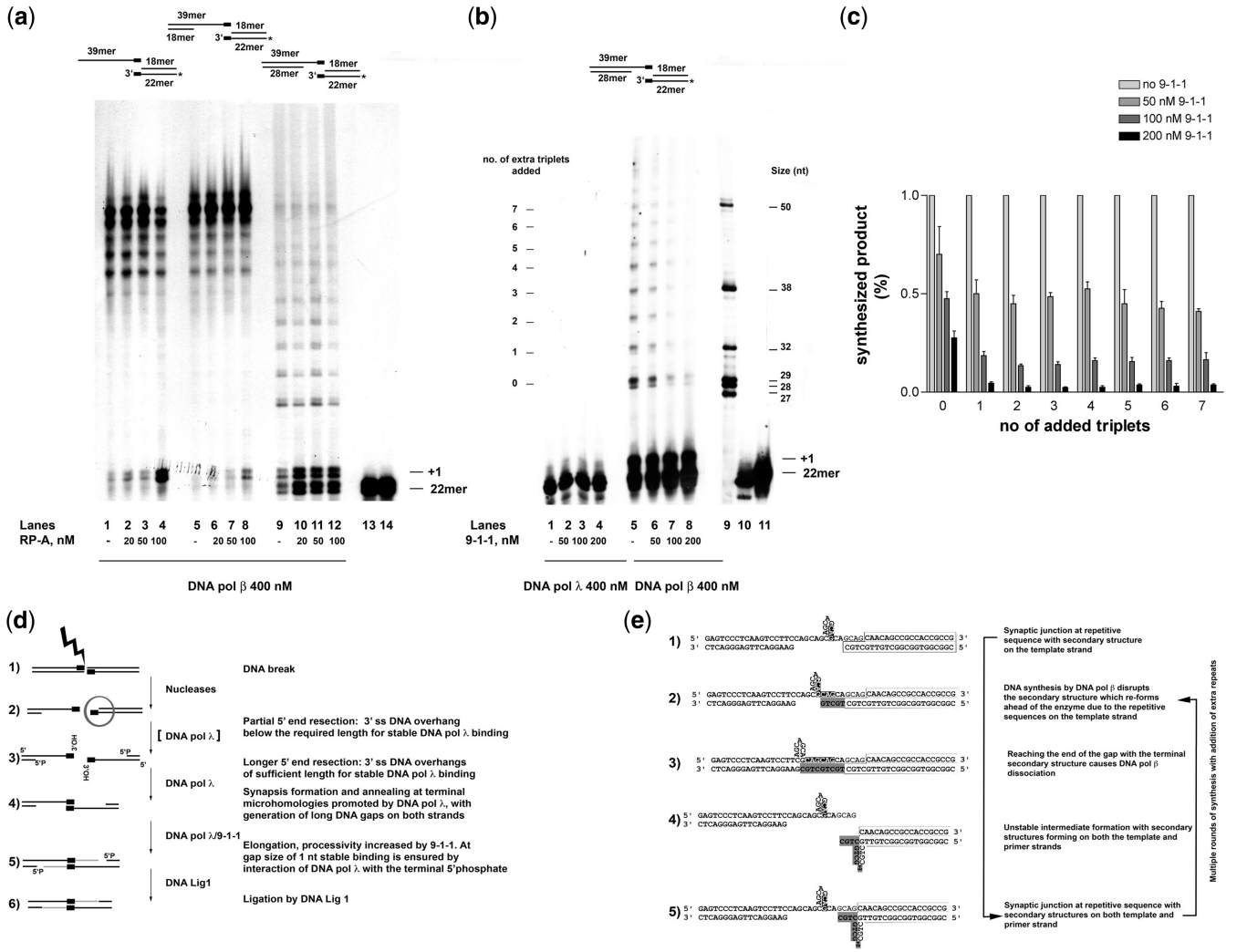

Figure 6. The Rad9/Hus1/Rad1 (9-1-1) complex reduces triplet expansion by DNA polymerase β. (**a**) DNA pol β was tested in the presence of 10 μM dNTPs and 50 nM of the 18/22-mer 'donor' template, 5′ labeled on the 22-mer strand, in combination with 50 nM of the 39-mer ss 'acceptor' oligonucleotide (lanes 1–4), or the 39/18 (lanes 5–8) or the 39/28 (lanes 9–12) 'acceptor' templates, in the absence (lanes 1, 5 and 9) or in the presence of increasing amounts of RP-A. Lanes 13, 14: control reactions in the absence of nucleotides. (**b**) DNA pol λ (lanes 1–4) or DNA pol β (lanes 5–8) were incubated in the presence of 10 μM dNTPs, 50 nM of the 18/22-mer 'donor' template, 5′ labeled on the 22-mer strand, in combination with 50 nM of the 39/28-mer 'acceptor' substrate and in the absence (lanes 1, 5) or in the presence of increasing amounts of 9-1-1. Lane 9: oligonucleotide size marker ladder. Lanes 10, 11: control reactions in the absence of dNTPs. (**c**) The bands representing extra triplet addition, as shown in the representative experiment presented in panel b, was quantified and the intensities relative to the value in the absence of 9-1-1 were plotted as a bar diagram. Values are the mean of measurements from three independent experiments. Error bars are ±S.D. (**d**) Proposed model for MMEJ by DNA pol λ. Upon DSB formation, nucleases generate 3′ ssDNA overhangs with terminal microhomology (step 1, black boxes), allowing stable synapsis formation by DNA pol λ at the microhomology regions and subsequent elongation assisted by the 9-1-1 complex and the 5′-phosphate of the terminal downstream nucleotide (steps 2–5). Upon completion of gap filling, DNA Ligase I seals the resulting nick (step 6). (**e**) Proposed model for triplet expansion during MMEJ promoted by DNA pol β. Triplet repeats form secondary structures (hairpin loops) on the template strand (step 1). During synthesis, DNA pol β can push these loops downstream (step 2), until the end of the gap, where the enzyme dissociates (step 3). Repetitive sequences can form secondary structures on both the primer and the template strand (step 4), before DNA pol β binds and promote a new round of synthesis (step 5). Iteration of steps 2–5 might lead to extensive triplet expansion at the junction.

annealing of two molecules with long ssDNA ends in a head-to-head fashion, exploiting the extensive self-complementarity existing between the CAG repeats (Figure 4). This was due to the intrinsic higher affinity of DNA pol λ for long ssDNA overhangs with respect to short ones. DNA pol β, on the other hand, did not show the same ability of DNA pol λ to promote annealing and elongation of long ssDNA 3′-overhangs bearing a single short microhomology region, consistent with the common notion that this enzyme is not involved in DSB repair in the majority of cell types. It was, however, able to promote annealing and elongation of short (5 nt) 3′ ssDNA overhangs, resulting, upon end joining, in a 1 nt-gap substrate. This suggested that DNA pol β might require a phosphorylated 5′-recessed end within a short distance from the 3′ ss overhang, for stable binding. Consistently with these findings, DNA pol β, contrary to DNA pol λ, was able to promote annealing of a short (4 nt) ss 3′-DNA overhang containing a single terminal GTC triplet, to complementary 3′ overhangs of different

lengths (7–39 nt), containing multiple CAG repeats, and could elongate them with similar efficiency (Table 2). However, copying of the repetitive CAG repeat sequence, generated products longer than the available template with a repetitive pattern of 3 nt addition, thus suggesting triplet expansion. The model proposed in Figure 6e, suggests that addition of extra copies of the CAG repeat results from the formation of secondary structures on both the template and the primer strand, during consecutive re-annealing and elongation steps. Consistent with the hypothesis that this mechanism involves only limited ssDNA tracts, RP-A did not show any effect. The 9-1-1 complex, on the other hand, appears to be able to significantly limit (but not completely suppress) the triplet expansion by DNA pol β. The model presented in Figure 6e predicts that the elongation step is highly distributive, involving frequent dissociation of the DNA pol from the template strand. This might also account for the requirement of high pol to DNA molar ratios (up to 10:1), in our *in vitro* assays, for MMEJ of DNA ends containing CAG repeats to occur. It is possible that additional factors contribute *in vivo* to stabilize the binding of the DNA pol to the synaptic complex between the DNA ends during the elongation step.

A possible role for DNA polymerase β- dependent MMEJ in triplet repeats expansion in HD

Somatic CAG triplet expansion in the Huntingtin gene is a molecular event linked to the development of the neurodegenerative Huntington's disease (HD) (34–36). Somatic CAG expansion increases with age and is tissue specific (37). In particular, it is highest in the brain region most commonly affected by HD, the striatum. It has been hypothesized that DNA pol β strand displacement DNA synthesis, during long-patch base excision repair in the context of repetitive sequences, generates 5′-flap structures that cannot be efficiently removed by the endonuclease Fen-1, whose expression is low in striatal neurons (38). Our data suggest that DNA pol β-mediated MMEJ repair of DSBs might be an additional mechanism responsible for triplet expansion in adult neurons.

Even though, so far, there is no direct evidence for an involvement of DNA pol β in DSBs repair, it is nevertheless possible to hypothesize a role of this DNA pol in both the repair of broken DNA ends through Ku-independent end joining pathways and the CAG triplet expansion in adult neurons, based on a number of considerations. First, NHEJ activity has been shown to decrease with aging due to decreased expression of Ku70 and Ku80 (39,40). Consistently with these findings, ss and ds DNA breaks have been documented to accumulate in neurons with age. Second, the age-dependent profile of the *in vitro* end-joining activity of extracts from rat cortical neurons revealed that post-mitotic neurons show maximum efficiency in joining ends with terminal homologies, but utilize an error-prone end-joining pathway to repair DSBs (41). Third, DNA pol β is the only DNA pol, which is significantly expressed in post-mitotic neurons. Fourth, mammalian DNA pol β was able to partially complement the NHEJ defect in a yeast strain lacking the family X DNA pol4, which has been proposed to be involved in yeast MMEJ (11). Interestingly, in such a system, DNA pol β activity was most efficient with DNA ends bearing a 4 nt terminal homology region. Finally, fifth and probably most relevant to this work, is the fact that a global map of human gene expression (42), indicated that in HD patients, two DNA pols were up-regulated (DNA pols β and ζ), five were down-regulated (DNA pols α, δ, ε, ι and λ) and two were unchanged (DNA pol η and Rev1). In view of the data presented here, it might be that up-regulation of DNA pol β is harmful, leading to an expansion of CAG repeats, which might be counteracted by the 9-1-1 complex. Since DNA pol β is the only family X DNA pol, which was found specifically overexpressed in HD patients, and chromatin immunoprecipitation experiments have shown that DNA pol β is significantly enriched at CAG expansion in the striatum tissue, but not in the cerebellum, of an HD mouse model animal (40), it would be, based on our results, of interest, to study the correlation between DNA pol β expression levels and DSBs repair during neuronal differentiation in general, and in the striatal neurons of HD patients.

SUPPLEMENTARY DATA

Supplementary Data are available at NAR Online: Supplementary Figures 1–2.

ACKNOWLEDGMENTS

We thank Dr. Elisa Zucca for critical reading of the manuscript.

FUNDING

This work was supported by the Swiss National Science Foundation (grant 31003A_133100/1) to U.H., Oncosuisse (grant KLS-02339-02-2009) to T.C, and University of Zürich to U.H. and in part to G.M. and by the Italian Association for Cancer Research AIRC IG12084 grant and the Superpig Program, project co-financed by Lombardy Region through the 'Fund for promoting institutional agreements' DGR5200/2007 to GM. Funding for open access charge: Italian Association for Cancer Research AIRC grant IG12084.

Conflict of interest statement. None declared.

REFERENCES

1. Symington,L.S. and Gautier,J. (2010) Double-strand break end resection and repair pathway choice. *Annu. Rev. Genet.*, **45**, 247–71, doi:10.1146/annurev-genet-110410-132435.
2. Fattah,F., Lee,E.H., Weisensel,N., Wang,Y., Lichter,N. and Hendrickson,E.A. (2010) Ku regulates the non-homologous end joining pathway choice of DNA double-strand break repair in human somatic cells. *PLoS Genet.*, **6**, e1000855.
3. McVey,M. and Lee,S.E. (2008) MMEJ repair of double-strand breaks (director's cut): deleted sequences and alternative endings. *Trends Genet.*, **24**, 529–538.

4. Ma,J.L., Kim,E.M., Haber,J.E. and Lee,S.E. (2003) Yeast Mre11 and Rad1 proteins define a Ku-independent mechanism to repair double-strand breaks lacking overlapping end sequences. *Mol. Cell. Biol.*, **23**, 8820–8828.
5. Taylor,E.M., Cecillon,S.M., Bonis,A., Chapman,J.R., Povirk,L.F. and Lindsay,H.D. (2010) The Mre11/Rad50/Nbs1 complex functions in resection-based DNA end joining in Xenopus laevis. *Nucleic Acids Res.*, **38**, 441–454.
6. Williams,G.J., Lees-Miller,S.P. and Tainer,J.A. (2010) Mre11-Rad50-Nbs1 conformations and the control of sensing, signaling, and effector responses at DNA double-strand breaks. *DNA Repair (Amst)*, **9**, 1299–1306.
7. Liang,L., Deng,L., Nguyen,S.C., Zhao,X., Maulion,C.D., Shao,C. and Tischfield,J.A. (2008) Human DNA ligases I and III, but not ligase IV, are required for microhomology-mediated end joining of DNA double-strand breaks. *Nucleic Acids Res*, **36**, 3297–3310.
8. Tseng,H.M. and Tomkinson,A.E. (2002) A physical and functional interaction between yeast Pol4 and Dnl4-Lif1 links DNA synthesis and ligation in nonhomologous end joining. *J. Biol. Chem.*, **277**, 45630–45637.
9. Tseng,H.M. and Tomkinson,A.E. (2004) Processing and joining of DNA ends coordinated by interactions among Dnl4/Lif1, Pol4, and FEN-1. *J. Biol. Chem.*, **279**, 47580–47588.
10. Lee,K. and Lee,S.E. (2007) Saccharomyces cerevisiae Sae2- and Tel1-dependent single-strand DNA formation at DNA break promotes microhomology-mediated end joining. *Genetics*, **176**, 2003–2014.
11. Daley,J.M., Laan,R.L., Suresh,A. and Wilson,T.E. (2005) DNA joint dependence of pol X family polymerase action in nonhomologous end joining. *J. Biol. Chem.*, **280**, 29030–29037.
12. Chan,S.H., Yu,A.M. and McVey,M. (2010) Dual roles for DNA polymerase theta in alternative end-joining repair of double-strand breaks in Drosophila. *PLoS Genet*, **6**, e1001005.
13. Yu,A.M. and McVey,M. (2010) Synthesis-dependent microhomology-mediated end joining accounts for multiple types of repair junctions. *Nucleic Acids Res.*, **38**, 5706–5717.
14. Hubscher,U., Maga,G. and Spadari,S. (2002) Eukaryotic DNA polymerases. *Annu. Rev. Biochem.*, **71**, 133–163.
15. Fan,W. and Wu,X. (2004) DNA polymerase lambda can elongate on DNA substrates mimicking non-homologous end joining and interact with XRCC4-ligase IV complex. *Biochem. Biophys. Res. Commun.*, **323**, 1328–1333.
16. Lee,J.W., Blanco,L., Zhou,T., Garcia-Diaz,M., Bebenek,K., Kunkel,T.A., Wang,Z. and Povirk,L.F. (2004) Implication of DNA polymerase lambda in alignment-based gap filling for nonhomologous DNA end joining in human nuclear extracts. *J. Biol. Chem.*, **279**, 805–811.
17. Paull,T.T. (2005) Saving the ends for last: the role of pol mu in DNA end joining. *Mol. Cell*, **19**, 294–296.
18. Capp,J.P., Boudsocq,F., Bertrand,P., Laroche-Clary,A., Pourquier,P., Lopez,B.S., Cazaux,C., Hoffmann,J.S. and Canitrot,Y. (2006) The DNA polymerase lambda is required for the repair of non-compatible DNA double strand breaks by NHEJ in mammalian cells. *Nucleic Acids Res.*, **34**, 2998–3007.
19. Capp,J.P., Boudsocq,F., Besnard,A.G., Lopez,B.S., Cazaux,C., Hoffmann,J.S. and Canitrot,Y. (2007) Involvement of DNA polymerase mu in the repair of a specific subset of DNA double-strand breaks in mammalian cells. *Nucleic Acids Res.*, **35**, 3551–3560.
20. Nick McElhinny,S.A., Havener,J.M., Garcia-Diaz,M., Juárez,R., Bebenek,K., Kee,B.L., Blanco,L., Kunkel,T.A. and Ramsden,D.A. (2005) A gradient of template dependence defines distinct biological roles for family X polymerases in nonhomologous end joining. *Mol. Cell*, **19**, 357–366.
21. Garcia-Diaz,M., Bebenek,K., Krahn,J.M., Blanco,L., Kunkel,T.A. and Pedersen,L.C. (2004) A structural solution for the DNA polymerase lambda-dependent repair of DNA gaps with minimal homology. *Mol. Cell*, **13**, 561–572.
22. Garcia-Diaz,M., Bebenek,K., Gao,G., Pedersen,L.C., London,R.E. and Kunkel,T.A. (2005) Structure-function studies of DNA polymerase lambda. *DNA Repair (Amst.)*, **4**, 1358–1367.
23. Moon,A.F., Garcia-Diaz,M., Batra,V.K., Beard,W.A., Bebenek,K., Kunkel,T.A., Wilson,S.H. and Pedersen,L.C. (2007) The X family portrait: structural insights into biological functions of X family polymerases. *DNA Repair (Amst.)*, **6**, 1709–1725.
24. Yamtich,J. and Sweasy,J.B. (2010) DNA polymerase family X: function, structure, and cellular roles. *Biochim. Biophys. Acta*, **1804**, 1136–1150.
25. Ramadan,K., Shevelev,I.V., Maga,G. and Hubscher,U. (2004) De novo DNA synthesis by human DNA polymerase lambda, DNA polymerase mu and terminal deoxyribonucleotidyl transferase. *J. Mol. Biol.*, **339**, 395–404.
26. Blanca,G., Shevelev,I., Ramadan,K., Villani,G., Spadari,S., Hübscher,U. and Maga,G. (2003) Human DNA polymerase lambda diverged in evolution from DNA polymerase beta toward specific Mn++ dependence: a kinetic and thermodynamic study. *Biochemistry*, **42**, 7467–7476.
27. Toueille,M., El-Andaloussi,N., Frouin,I., Freire,R., Funk,D., Shevelev,I., Friedrich-Heineken,E., Villani,G., Hottiger,M.O. and Hubscher,U. (2004) The human Rad9/Rad1/Hus1 damage sensor clamp interacts with DNA polymerase beta and increases its DNA substrate utilisation efficiency: implications for DNA repair. *Nucleic Acids Res.*, **32**, 3316–3324.
28. Maga,G., Ramadan,K., Locatelli,G.A., Shevelev,I., Spadari,S. and Hubscher,U. (2005) DNA elongation by the human DNA polymerase lambda polymerase and terminal transferase activities are differentially coordinated by proliferating cell nuclear antigen and replication protein A. *J. Biol. Chem.*, **280**, 1971–1981.
29. Parrilla-Castellar,E.R., Arlander,S.J. and Karnitz,L. (2004) Dial 9-1-1 for DNA damage: the Rad9-Hus1-Rad1 (9-1-1) clamp complex. *DNA Repair (Amst.)*, **3**, 1009–1014.
30. Helt,C.E., Wang,W., Keng,P.C. and Bambara,R.A. (2005) Evidence that DNA damage detection machinery participates in DNA repair. *Cell Cycle*, **4**, 529–532.
31. Smirnova,E., Toueille,M., Markkanen,E. and Hubscher,U. (2005) The human checkpoint sensor and alternative DNA clamp Rad9-Rad1-Hus1 modulates the activity of DNA ligase I, a component of the long-patch base excision repair machinery. *Biochem. J.*, **389**, 13–17.
32. Gembka,A., Toueille,M., Smirnova,E., Poltz,R., Ferrari,E., Villani,G. and Hubscher,U. (2007) The checkpoint clamp, Rad9-Rad1-Hus1 complex, preferentially stimulates the activity of apurinic/apyrimidinic endonuclease 1 and DNA polymerase beta in long patch base excision repair. *Nucleic Acids Res.*, **35**, 2596–2608.
33. Meister,P., Poidevin,M., Francesconi,S., Tratner,I., Zarzov,P. and Baldacci,G. (2003) Nuclear factories for signalling and repairing DNA double strand breaks in living fission yeast. *Nucleic Acids Res.*, **31**, 5064–5073.
34. McFarland,K.N. and Cha,J.H. (2011) Molecular biology of Huntington's disease. *Handb. Clin. Neurol.*, **100**, 25–81.
35. Margolis,R.L., McInnis,M.G., Rosenblatt,A. and Ross,C.A. (1999) Trinucleotide repeat expansion and neuropsychiatric disease. *Arch. Gen. Psychiatry*, **56**, 1019–1031.
36. Monckton,D.G. and Caskey,C.T. (1995) Unstable triplet repeat diseases. *Circulation*, **91**, 513–520.
37. Pearson,C.E., Nichol Edamura,K. and Cleary,J.D. (2005) Repeat instability: mechanisms of dynamic mutations. *Nat. Rev. Genet.*, **6**, 729–742.
38. Liu,Y., Prasad,R., Beard,W.A., Hou,E.W., Horton,J.K., McMurray,C.T. and Wilson,S.H. (2009) Coordination between polymerase beta and FEN1 can modulate CAG repeat expansion. *J. Biol. Chem.*, **284**, 28352–28366.
39. Vyjayanti,V.N. and Rao,K.S. (2006) DNA double strand break repair in brain: reduced NHEJ activity in aging rat neurons. *Neurosci. Lett.*, **393**, 18–22.
40. Goula,A.V., Berquist,B.R., Wilson,D.M. III, Wheeler,V.C., Trottier,Y. and Merienne,K. (2009) Stoichiometry of base excision repair proteins correlates with increased somatic CAG instability in striatum over cerebellum in Huntington's disease transgenic mice. *PLoS Genet.*, **5**, e1000749.
41. Rao,K.S. (2007) DNA repair in aging rat neurons. *Neuroscience*, **145**, 1330–1340.
42. Lukk,M., Kapushesky,M., Nikkilá,J., Parkinson,H., Goncalves,A., Huber,W., Ukkonen,E. and Brazma,A. (2010) A global map of human gene expression. *Nat. Biotechnol.*, **28**, 322–324.